

Effective field approach for long-range dissolved DNA polymer dynamics

V. K. Saxena,* L. L. Van Zandt, and W. K. Schroll

Department of Physics, Purdue University, West Lafayette, Indiana 47906

(Received 17 June 1988; revised manuscript received 22 September 1988)

Long-range interatomic interactions between distant parts of a DNA helix are known to be dominant factors in determining longitudinal DNA motions. A local field approach has been developed to account for these long-range forces that both simplifies the numerical complications involved in the previous treatment of these interactions and rationalizes the physics. The method leads to excellent agreement with the experimental value for the speed of longitudinal sound (≈ 2.0 km/s), where agreement was the chief virtue of the earlier method. A new result of this theory is the prediction of one-dimensional plasmon excitations, analogous to plasmons in higher-dimensional charged systems. This one-dimensional plasmon has an electromagnetic character in contrast to the mostly mechanical nature of the slower compressional sound-wave phonon modes. The dispersion for this plasmon mode is soundlike, having a speed of propagation of some 36.0 km/s. Analysis of the effect of viscous frictional forces shows that the one-dimensional plasmon waves are well-defined resonant states for parameter values where the mechanical phonon modes are strongly overdamped.

I. INTRODUCTION

We have long been interested in the mechanical behavior of a DNA polymer chain. The problem of determining the vibrational behavior of a DNA chain under various conditions and perturbations has been a staple calculation in our group (as well as a number of others) for some time. The importance of long-range interatomic interactions, particularly for the low-frequency portion of the DNA vibrational spectrum was discovered by Mei *et al.* in the 1980.¹ These authors determined that contributions to the interatomic potentials from base pairs at least 15 to 20 units away ($> 60\text{\AA}$) were non-negligible for computing the velocity of longitudinal sound as well as other concomitant changes in the normal-mode spectrum. Mei *et al.*¹ used absolute values of charges on the constituent atoms, based on the argument of mechanical stability of the crystal, in evaluating the interatomic long-range potentials.

The determination of the low-amplitude vibrational behavior of a molecular system involves the setting up and diagonalization of a "force constant matrix:" the solution of the algebraic problem

$$\sum_j (D_{i,j} - \omega^2 I) q_j = 0. \quad (1)$$

In this $D_{i,j}$ describes the force on atom i caused by a perturbation from equilibrium position of atom j ; I is the unit matrix. That as many as 40 base pairs of 123 degrees of freedom each contribute, demands that over 30 000 coefficients be dealt with in some fashion or other. For most calculations, we have used the symmetries of a homopolymer model to reduce the algebraic problem to a manageable 123×123 $D_{i,j}$'s, but the individual coefficients each still includes > 60 contributions that must first be evaluated prior to the diagonalization process.

The symmetry-driven simplification breaks down for the problem of localized, symmetry-breaking modifications of the structure. An example of this is an

end to the chain. An attempt was made to treat the broken symmetry problem by Putnam *et al.*² but the only way this calculation could be carried out was by simply dropping the long-range terms. One cannot place great credence in the numerical results of such an uncontrolled approximation. Nonetheless, the problem is an important one in that biological activity is a property of heterogeneous polymers, the symmetry is broken in a variety of ways. Hence we persist in a search for a satisfactory simple method of including long-range forces.

We describe here a substantial reduction of the problem complexity in which we exploit the physical fact that these multiple interactions are largely Coulombic in origin. While the exact distance dependence could not be pinned down by the arguments in Ref. 1, it was established that the forces depend on a very low inverse power of atomic separation. This, and the fact that because of the partial charges on the constituent DNA atoms we know there must exist long-range Coulomb interactions, makes it reasonable to attempt to describe the many long-range terms as purely electrical.

To this end, we explicitly introduce the longitudinal electric field. The force on atom i is then determined by a single physical parameter. The electric field itself is found from treating the partially charged atoms as its sources. At first sight it would seem we have gained little by this strategy. However, the electric field and the dielectrical polarization obey the *local* relation

$$\nabla \cdot \mathbf{E} = - \frac{1}{\epsilon_{in}} \nabla \cdot \mathbf{P} \quad (2)$$

and \mathbf{P} can be directly related to the atomic displacements [cf. Eq. (52) below].

The relation between \mathbf{P} and \mathbf{E} is not especially simple, turning out to be frequency and wavelength dependent. The complications are introduced by the electrostatics of \mathbf{E} and \mathbf{B} as they extend into the surrounding solvent. An interesting additional feature of the system that we have emphasized in another article³ is the appearance of

a new class of elementary excitations, the one-dimensional plasmons. These modes are dominantly of electromagnetic character, in contrast to the mechanical waves predicted by Eq. (1) when \mathbf{E} is not explicitly incorporated. They are analogous to the well-known bulk and surface plasmons of metal and plasma physics while showing modifications consequential to their lower dimensionality in DNA.

The observability of these new plasmon modes hinges on the question of the damping to be expected for them. It is useful to contrast their behavior with that of the similar, lower-frequency compressional waves in this regard. Simple hydrodynamic considerations⁴ suggest that longitudinal sound should be overdamped and unobservable, and although there has been a report of its observation,⁵ other workers have been unable to confirm this.⁶ Hence in the example calculations of this work, we assumed values for the viscous damping parameters that led to overdamped sound. For this parameter set, the plasmons are found to be well-defined resonant states. The reason for the difference, even though both types of waves involve longitudinal displacements, is that the plasmons are mostly electromagnetic in character. That is, for a given $\hbar\omega$, a greater fraction of plasmon energy appears as $\epsilon E^2 + B^2/\mu_0$ and only a small part as mechanical kinetic energy subject to damping loss.

Before proceeding to the calculational details, we consider the model of the polymer in solvent. Equation (1), modified by inclusion of E_z , is appropriate to dry DNA in vacuum; in solution, a sheath of water and positive ions surrounds the polymer (cf. Fig. 1). Regardless of the overall ionic strength of the solvent, the counterion concentration in this sheath will lie somewhere around $5M$ (for monovalent cations); this is sufficient effectively to neutralize the DNA charge density in about 5 \AA or less, not much farther than a single H_2O monolayer. A complete Poisson-Boltzmann computation of ion densities around DNA was presented by Davis and Van Zandt.⁷ The water-ion sheath is considerably modified in its prop-

erties by the polymer within, as Tao *et al.*⁸ have shown. Hence we use a separate coordinate $s(z, t)$ to describe the near-water longitudinal motion. This "counterion sheath" coordinate is included in the equations of motion together with 123 coordinates of Eq. (1). We actually need to know relatively little about the sheath water dynamics; it has an internal elasticity for which we assume the same values as bulk water, a linear charge density λ that we take as equal and opposite to that of the DNA, and viscoelastic coupling constants to the inner DNA and the outer bulk solvent. The inner coupling we adjust to overdamp the mechanical sound, and the outer coupling we set to match bulk-water/water viscosity. When we got to calculate the polarization density \mathbf{P} we include 3.4 \AA of sheath material with each base pair.

Longitudinal motion is thus undertaken by both DNA polymer and sheath solvent. These materials are oppositely charged. For the modes in which both oscillate in phase, detailed local charge neutrality is largely maintained and little electric polarization takes place; this is mechanical sound with a velocity of about 2 km/sec . In the plasmon case, the phase of polymer and sheath material motion is opposite; a large electric polarization arises as positive sheath goes one way and the negative DNA goes the other, the restoring forces are dominated by the electric "stiffness," and a much higher sound velocity results, some 36 km/sec .

We have restricted the present calculation to the case where the electromagnetic fields drop to zero at large distances. The shape of the plasmon spectrum depends on this in a crucial way, as we have mentioned. This is also the high hydration, infinite dilution limit. To back away from this limit in order to consider partially hydrated, dense DNA systems would require modeling the three-dimensional structure of tangled, interacting polymer chains and result in a proliferation of adjustable parameters. Given the present experimental situation of so few established points, this extension would be unproductive.

In Sec. II we present the equations of motion for the DNA-sheath-counterion system. The details of the calculation of the effective local electric field are discussed in Sec. III. Section IV describes the parameter values used in our calculations and the mathematical procedure utilized to obtain the low-frequency vibrational modes of the system. In Sec. V we present our conclusions and a discussion of our results.

II. EQUATIONS OF MOTION

In this section we develop the equations of motion for the DNA polymer in the presence of the counterion sheath, first writing the equation of motion for the dry molecule. By taking advantage of the helical symmetry of the DNA, the equations of motion can be reduced to a set of equations for atoms within a unit cell. Thus within the harmonic approximation, the equations of motion of the dry molecule, in Cartesian coordinates, can be written as^{9,10}

$$m_i \frac{\partial^2 r_i^\alpha}{\partial t^2} = \sum_{j,\beta} F_{i,j}^{\alpha\beta} \delta r_j^\beta, \quad (3)$$

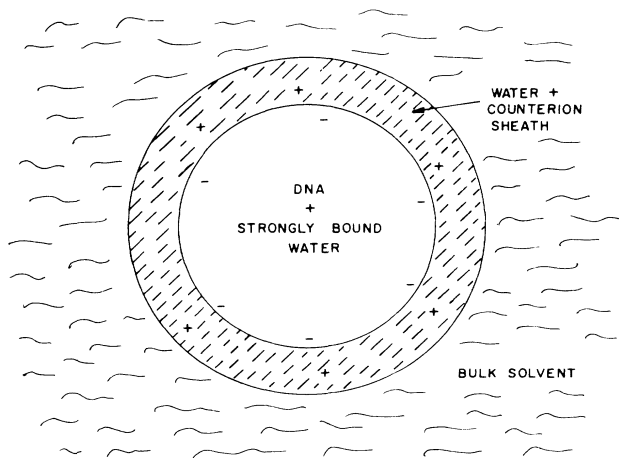


FIG. 1. Schematic of approximately cylindrical "dry" DNA polymer, surrounded by a structurally modified sheath of ion containing water, the "hydration layer," all immersed in solvent ocean. We see here a slab cut transversely to the long axis of the system, one slice from a long "loaf."

where m_i is the mass and r_i^α is the coordinate α ($=x, y, z$) of atom i in the unit cell and δr_i^α is the corresponding displacement. $F_{i,j}^{\alpha\beta}$ is the force constant matrix for the dry molecule.

In order to account for the presence of counterions and the charges on the distant parts of the molecule we recognize that there is an electric field E_z in the z direction, which is taken as the helix axis. This dynamic electric field arises from the atomic motions of the DNA and the motion of its counterions, and is in turn coupled to the charges in the system. In the presence of this electric field E_z the equation of motion of the molecule becomes

$$m_i \frac{\partial^2 r_i^\alpha}{\partial t^2} = \sum_{j,\beta} F_{i,j}^{\alpha\beta} \delta r_j^\beta + e_i E_z ; \quad (4)$$

e_i is the partial charge on atom i . We are ignoring the small radial components of \mathbf{E} from the distant charges.

Counterions interact strongly with the solvent and effectively there is no relative motion on the time scale of interest in microwave absorption experiments. Furthermore, the counterion distribution density is large within the range of the first water monolayer and decays very fast as we go away from the helix axis. Therefore we assume that the total charge of the counterions is contained within the counterion sheath. The sheath is most strongly coupled to the phosphate-group atoms in the backbone. We assign a single dynamical coordinate s to the local sheath longitudinal displacement. This coordinate is assumed to represent the motion, along the z axis, of the water and the counterions of the sheath. The equation of motion for the variable s can be written as

$$a\rho \frac{\partial^2 s}{\partial t^2} = a\rho v_w^2 \frac{\partial^2 s}{\partial z^2} - \lambda_{dc} E_z , \quad (5)$$

where ρ is the linear mass density of the sheath and a is the linear pitch of the DNA helix. v_w is the speed of sound in the sheath water. $-\lambda_{dc}$ is the total charge on the counterions within the sheath ($\lambda_{dc} = \sum_i e_i$). For simplicity we have assumed complete charge neutrality within the sheath outer radius, and therefore have assigned the amount of charge on the counterions to be exactly equal and opposite to the total charge on the DNA molecule.

The coupling of the water of the sheath to the molecule is considered as a frictional interaction, contributing a term $(\dot{s} - \dot{r}_i^z)\Gamma$ in the equation of motion for the atom i . We assume a simplified coupling between the z -component motion of the surface atoms and the sheath, and no coupling with the x and y components. Finally, a second frictional coupling is assumed between the sheath and the bulk water, giving a force term $-\gamma\dot{s}$ in the equation of motion for the variable s . Collecting all these terms, the equations of motion for the molecule and the water shell-counterion system can be written as

$$m_i \frac{\partial^2 r_i^\alpha}{\partial t^2} = \sum_{j,\beta} F_{i,j}^{\alpha\beta} \delta r_j^\beta + e_i E_z + \Gamma(\dot{s} - \dot{r}_i^z) \delta_{ip} \delta_{\alpha z} \quad (6)$$

and

$$a\rho \frac{\partial^2 s}{\partial t^2} = a\rho v_w^2 \frac{\partial^2 s}{\partial z^2} - \lambda_{dc} E_z + \sum_{\text{phosphate group}} \Gamma(\dot{r}_i^z - \dot{s}) + \gamma\dot{s} , \quad (7)$$

where δ_{ip} is 1 if i is a phosphate group atom and 0 otherwise. $\delta_{\alpha z}$ restricts the coupling only to the z component of the velocity of the phosphate group atoms. Assuming harmonic time dependence of the form $\exp(-i\omega t)$ and using the mass-weighted coordinates $q_i^\alpha = \sqrt{m_i} \delta r_i^\alpha$ and $\bar{s} = \sqrt{a\rho s}$, Eqs. (6) and (7) are reduced to

$$-\omega^2 q_i^\alpha = \sum_{j,\beta} D_{ij}^{\alpha\beta} q_j^\beta + e'_i E_z - i\omega \Gamma_i (\bar{s} - q_i^\alpha \eta_i) \delta_{ip} \delta_{\alpha z} \quad (8)$$

and

$$-\omega^2 \bar{s} = -k^2 v_w^2 \bar{s} - \lambda'_{dc} E_z - i\omega \sum_i \Gamma_i (q_i^z - \bar{s} / \eta_i) \delta_{ip} - i\omega \gamma' \bar{s} , \quad (9)$$

where $e'_i = e_i / \sqrt{m_i}$, $\lambda'_{dc} = \lambda_{dc} / \sqrt{a\rho}$, $\gamma' = \gamma / a\rho$, $\eta_i = \sqrt{a\rho / m_i}$,

$$D_{ij}^{\alpha\beta} = F_{ij}^{\alpha\beta} / \sqrt{m_i m_j} , \quad (10)$$

and

$$\Gamma_i = \Gamma / \sqrt{a\rho m_i} . \quad (11)$$

We will use these equations of motion in Sec. IV to calculate the phonon spectrum of the system, where we will also discuss the numerical values of various parameters used in the calculations.

III. ELECTRIC FIELD

In this section we calculate the effective internal field E_z . We adopt a cylindrical model of DNA and the sheath, as has been used by Dorfman and Van Zandt⁴ and Davis and Van Zandt.⁷ Within the outer radius r_1 of the sheath, the total electric field \mathbf{E} is given by

$$\mathbf{E} = -\frac{\mathbf{P}}{\epsilon_{in}} + \mathbf{E}_1 , \quad (12)$$

where \mathbf{P} is the electric polarization generated by the displacements of the DNA atoms and the counterions, and ϵ_{in} is the average dielectric constant within the cylindrical region of the DNA and the sheath. The contribution of the electric polarization \mathbf{P} to the internal electric field is confined to the radius of the sheath. To account for any other contribution to the electric field inside or outside r_1 , we introduce an extra field term \mathbf{E}_1 , which must have zero divergence, i.e.,

$$\nabla \cdot \mathbf{E}_1 = 0 . \quad (13)$$

We are assuming that there is no free charge density outside of that accounted for by \mathbf{P} .

Since in the microwave region we are mainly interested in the longitudinal modes of the system, as a simplifying assumption, we consider the electric polarization to lie only along the z direction, and therefore set

$$\nabla \cdot \mathbf{P} = \frac{\partial P_z}{\partial z} . \quad (14)$$

The polarization and the electromagnetic fields propagate along the helix axis as harmonic disturbances. Assuming an infinite helix, the electric fields \mathbf{E} and \mathbf{E}_1 should satisfy the following boundary conditions at the ends of the polymer:

$$\mathbf{E}_1(z = -\infty) = \frac{\mathbf{P}}{\epsilon_{\text{in}}} \quad (15)$$

and

$$\mathbf{E}(z = \pm\infty) = 0. \quad (16)$$

Applying Gauss's law to the regions inside and outside of the radius r_1 gives the following relations among the electric field components:

$$\frac{\partial E_z^{(\text{in})}}{\partial z} + \frac{2}{r_1} E_r^{(\text{in})} = -\frac{1}{\epsilon_{\text{in}}} \frac{\partial P}{\partial z} \quad (17)$$

and

$$\frac{\partial E_z^{(\text{out})}}{\partial z} + \frac{2}{r_1} E_r^{(\text{out})} = 0. \quad (18)$$

Continuity of the electric displacement normal to the surface of the cylinder gives the following boundary condition:

$$\epsilon_{\text{out}} E_r^{(\text{out})} - \epsilon_{\text{in}} E_r^{(\text{in})} = \frac{\lambda}{2\pi r_1}, \quad (19)$$

where λ is the time dependent part of the polymer-counterion charge density. Using the definition of current density as $\mathbf{j} = \sigma \mathbf{E}$, where σ is the electrical conductivity of the solvent, and using the relation (charge conservation)

$$\frac{\lambda}{2\pi r_1} = \int_0^t (-\mathbf{j} \cdot \hat{\mathbf{n}}) dt, \quad (20)$$

where $\hat{\mathbf{n}}$ is the unit vector normal to the surface of the cylinder, one gets

$$\frac{\dot{\lambda}}{2\pi r_1} = -\sigma E_r^{(\text{out})}. \quad (21)$$

Taking time derivative of Eq. (19) and using Eq. (21), the boundary condition at the surface of the cylinder can be expressed as

$$\epsilon_{\text{out}} \dot{E}_r - \epsilon_{\text{in}} \dot{E}_r^{(\text{in})} = -\sigma E_r. \quad (22)$$

The continuity of the tangential component of the electric field at the surface of the cylinder leads to the condition

$$E_z^{(\text{in})} = E_z^{(\text{out})} \equiv E_z. \quad (23)$$

Taking the time derivative of Gauss's law, Eq. (17), and using Eq. (23), one gets another relation between the components of the electric field

$$\frac{\partial \dot{E}_z}{\partial z} + \frac{2}{r_1} \dot{E}_r^{(\text{in})} = -\frac{1}{\epsilon_{\text{in}}} \frac{\partial \dot{P}}{\partial z}. \quad (24)$$

We now proceed to calculate E_1 in terms of E . Using the cylindrical symmetry of the system we assume the

electric fields and the polarization to be independent of the azimuthal angle θ . The component E_θ of the electric field is assumed to be constant, and can be taken as zero. Thus Maxwell's equations for the electric field can be written as

$$\nabla \cdot \mathbf{E} = \frac{\partial E_z}{\partial z} + \frac{E_r}{r} + \frac{\partial E_r}{\partial r} = 0, \quad (25)$$

$$\nabla \times \mathbf{E} = \hat{\theta} \left[\frac{\partial E_r}{\partial z} - \frac{\partial E_z}{\partial r} \right] - \dot{\mathbf{B}}. \quad (26)$$

Due to the cylindrical symmetry and assumed properties of the electric field the magnetic induction \mathbf{B} has only the θ component: $\mathbf{B} = \hat{\theta} B_\theta = \hat{\theta} B$. Thus Eq. (26) takes the form

$$\dot{B} = \frac{\partial E_z}{\partial r} - \frac{\partial E_r}{\partial z} = -\frac{\partial B}{\partial z} v, \quad (27)$$

where we have assumed the propagation of a disturbance of the form $f(z - vt)$, v being the speed of propagation of the disturbance through the system along the helix axis.

Ampere's law, applied to the system, leads to

$$\hat{r} \left[-\frac{\partial B}{\partial z} \right] + \hat{z} \left[\frac{\partial B}{\partial r} + \frac{B}{r} \right] = \mu_0 (\sigma \mathbf{E} + \epsilon \dot{\mathbf{E}}). \quad (28)$$

By separating the \hat{r} and \hat{z} components of Eq. (28) and using Eq. (27) we obtain

$$\frac{1}{v} \left[\frac{\partial E_z}{\partial r} - \frac{\partial E_r}{\partial z} \right] = \mu_0 (\sigma E_r + \epsilon \dot{E}_r) \quad (29)$$

and

$$\frac{\partial B}{\partial r} + \frac{B}{r} = \mu_0 (\sigma E_z + \epsilon \dot{E}_z). \quad (30)$$

Taking a partial radial derivative of the divergence equation $\nabla \cdot \mathbf{E} = 0$, one gets

$$\frac{\partial}{\partial z} \frac{\partial E_z}{\partial r} + \frac{1}{r} \frac{\partial E_r}{\partial r} - \frac{1}{r^2} E_r + \frac{\partial^2 E_r}{\partial r^2} = 0. \quad (31)$$

The partial z derivative of Eq. (29) gives us

$$\frac{1}{v\mu_0} \left[\frac{\partial^2 E_z}{\partial r \partial z} - \frac{\partial^2 E_r}{\partial z^2} \right] = \sigma \frac{\partial E_r}{\partial z} + \epsilon \frac{\partial \dot{E}_r}{\partial z}. \quad (32)$$

Eliminating $\partial^2 E_z / \partial r \partial z$ between Eqs. (31) and (32) and using the identity

$$\frac{\partial \dot{E}_r}{\partial z} = -v \frac{\partial^2 E_r}{\partial z^2}, \quad (33)$$

one gets the following relation for the component E_r :

$$\frac{\partial^2 E_r}{\partial r^2} + \frac{1}{r} \frac{\partial E_r}{\partial r} - \frac{1}{r^2} E_r + (1 - \epsilon\mu_0 v^2) \frac{\partial^2 E_r}{\partial z^2} + \sigma\mu_0 v \frac{\partial E_r}{\partial z} = 0. \quad (34)$$

Taking time derivative of Eq. (30), using Eq. (27) and finally utilizing Eq. (25) one obtains

$$\frac{\partial^2 E_z}{\partial r^2} + \frac{\partial^2 E_z}{\partial z^2} + \frac{1}{r} \frac{\partial E_z}{\partial r} = \mu_0(\sigma \dot{E}_z + \epsilon \ddot{E}_z). \quad (35)$$

Once again using the time dependence $f(z - vt)$ for the field component E_z , one obtains from Eq. (35)

$$\frac{\partial^2 E_z}{\partial r^2} + \frac{1}{r} \frac{\partial E_z}{\partial r} + (1 - \epsilon \mu_0 v^2) \frac{\partial^2 E_z}{\partial z^2} + \sigma \mu_0 v \frac{\partial E_z}{\partial z} = 0. \quad (36)$$

Keeping in mind the boundary conditions Eqs. (15) and (16), we can Fourier transform, with respect to the variable z the electric field components E_r and E_z , as

$$E_r = \int_{-\infty}^{\infty} E_r(q) e^{iq(z-vt)} dq \quad (37)$$

and

$$E_z = \int_{-\infty}^{\infty} E_z(q) e^{iq(z-vt)} dq, \quad (38)$$

where q is the wave vector for the disturbance propagating along the helix axis. By applying the Fourier transform to Eq. (36) we obtain

$$\frac{\partial^2 E_z(q)}{\partial r^2} + \frac{1}{r} \frac{\partial E_z(q)}{\partial r} + q^2 \left[1 - \epsilon \mu_0 v^2 + i \frac{\sigma \mu_0 v}{q} \right] E_z(q) = 0, \quad (39)$$

which is Bessel's equation. Thus

$$E_z(q) = E_0(q) H_0(\kappa r), \quad (40)$$

where $H_0(\kappa r)$ is the zeroth-order Hankel function and

$$\kappa^2 = q^2 \left[1 - \epsilon \mu_0 v^2 + i(\sigma \mu_0 v / q) \right]. \quad (41)$$

Similarly Fourier transforming Eq. (34) leads, for the radial part of the electric field, to

$$\frac{\partial^2 E_r(q)}{\partial r^2} + \frac{1}{r} \frac{\partial E_r(q)}{\partial r} - \frac{1}{r^2} E_r(q) + q^2 \left[1 - \epsilon \mu_0 v^2 + i \frac{\sigma \mu_0 v}{q} \right] E_r(q) = 0, \quad (42)$$

which has a solution

$$E_r(q) = E_1(q) H_1(\kappa r), \quad (43)$$

where $H_1(\kappa r)$ is the first-order Hankel function.

Now applying the Fourier transform to the boundary condition, Eq. (22), and using the above solution for $E_r(q)$, one gets

$$E_r^{(in)}(q) = \frac{i \epsilon_{out} q v - \sigma}{i \epsilon_{in} q v} E_1(q) H_1(\kappa r_1). \quad (44)$$

From the divergence theorem for the electric field, using the solutions for E_z and E_r one obtains

$$E_1(q) = -i(q/\kappa) E_0(q). \quad (45)$$

Using Eqs. (44) and (45) finally we get for the field $E_r^{(in)}(q)$ as

$$E_r^{(in)}(q) = -i \frac{q}{\kappa} \frac{\epsilon_{out} + i\sigma/qv}{\epsilon_{in}} E_0(q) H_1(\kappa r_1). \quad (46)$$

Fourier transforming Eq. (24), substituting solutions for E_r and E_z , and finally using Eq. (46) for $E_r^{(in)}$, one obtains the final expression for the electric field amplitude $E_0(q)$:

$$E_0(q) = \frac{P(q)}{E_{in}} \left[2 \frac{\epsilon_{out} + i\sigma/qv}{\epsilon_{in}} \frac{H_1(\kappa r_1)}{\kappa r_1} - H_0(\kappa r_1) \right]^{-1}, \quad (47)$$

where $P(q)$ is the Fourier transform of the electric polarization P_z . The electric field E_z is finally given as

$$E_z(\omega) = \frac{1}{\epsilon_{in}} \omega P(\omega) H_0(\kappa r_1) \times \left[\frac{i\sigma + \omega \epsilon_{out}}{\epsilon_{in}} \frac{2H_1(\kappa r_1)}{\kappa r_1} - \omega H_0(\kappa r_1) \right]^{-1}. \quad (48)$$

For the low-frequency modes near the zone center (i.e., for small values of q), one can expand E_z in powers of q , using the asymptotic forms for H_0 and H_1 in the limit $q \rightarrow 0$, as a reasonable approximation. For $q \rightarrow 0$, $\kappa^2 \approx iq\sigma\mu_0v$, and in this limit the functions H_0 and H_1 behave as

$$H_0(q \rightarrow 0) \approx \frac{2}{\pi} \ln \kappa r_1 \quad (49)$$

and

$$H_1(q \rightarrow 0) \approx \frac{2}{\pi \kappa r_1}. \quad (50)$$

Using these asymptotic forms in E_z , the leading term in the asymptotic expansion of the electric field give us

$$E_z \approx \frac{1}{2} P_z \mu_0 v^2 q^2 r_1^2 \ln[r_1(\sigma \mu_0 v q)^{1/2}]. \quad (51)$$

In terms of the atomic displacements q_i^z and the coordinates \bar{s} the electric polarization can be written as

$$P_z = \frac{1}{\pi r_1^2 a} \left[\sum_i e'_i q_i^z - \lambda'_{dc} \bar{s} \right]. \quad (52)$$

Using Eq. (52) for P_z we can carry E_z from Eq. (51) back into Eqs. (8) and (9) to get a set of coupled equations in the dynamical variables q_i^z and \bar{s} alone, which can then be solved for the vibrational models of the system in the usual fashion. The q^2 dependence of E_z in Eq. (51) and the substitution of E_z in the equations of motion indicate that the effect of the dynamic electric field on the spectrum of the system should lead to a mode, in the low-frequency limit, with the frequency linearly dependent on the wave vector q . Thus the inclusion of the effect of dynamic electric field is expected to give rise to an acoustic-type mode, with a linear q dependence plus a very weak logarithmic singularity at very small q . It is known that the vibrational spectrum of dry DNA, at the zone center, exhibits two acoustic modes. Our examination here of the equations of motion of the system, including the effect of the dynamic electric field, indicates the existence of an extra acoustic-type mode at the zone

center. We verify this by numerical calculations presented in Sec. IV.

IV. CALCULATION AND RESULTS

In this section we will discuss various parameters and the forms of the damping constants Γ and γ used in our calculations. We will also outline the method of calculation and present the numerical results for the low-frequency modes of the DNA-sheath system.

The force constant matrix $F_{ij}^{\alpha\beta}$ is constructed,¹⁰ in the Cartesian coordinate system, by starting from internal force constants for bond stretch, angle bend, and twist for the bonded interactions, then making a transformation from internal coordinates to Cartesian coordinates. The nonbonded long-range electrostatic interactions are mainly accounted for by E_z , but are specifically included for atomic pairs within the unit cell. Some further long-range electrostatic interactions between atoms in the central unit cell and the nearest-neighbor cells on both sides are also included explicitly in the matrix $F_{ij}^{\alpha\beta}$. These forces tend to stiffen the polymer chain. In evaluating these long-range electrostatic interactions we, like Mei *et al.*,¹ use the absolute values of the charges on the atoms.

The damping constant Γ for the coupling between the DNA and the sheath has been discussed by Davis and Van Zandt.⁷ We use their form here:

$$\Gamma = \frac{2\pi r_0 G \eta}{(r_1 - r_0)(1 - i\omega\tau_1)}, \quad (53)$$

where r_0 is the radius of the DNA (assuming a cylindrical form), η is the zero-frequency shear viscosity of water, taken as 0.01 P. τ_1 is the relaxation time for the sheath, taken to be 4×10^{-11} s from the results of Tao *et al.*, G is a numerical factor which accounts for the number and geometrical orientation of the bonds across the DNA-sheath interface. Values for G have been discussed by Davis and Van Zandt⁷ and it was found that a value of $G = 0.02$ can be reasonably justified. We have used this value of G in our calculations.

The force constant γ the coupling between the sheath and the bulk water is taken to be

$$\gamma = \frac{2\pi r_1 \eta}{1 - i\omega\tau_2}, \quad (54)$$

where τ_2 is the relaxation time for the bulk water, taken to be $\tau_2 = 10^{-12}$ s.

The speed of sound v_w in Eq. (5) was taken to be 1.5×10^3 m/s, as for the bulk water. The conductivity of the solvent σ was taken to be 1.0×10^{-2} mho/m, corresponding to a 5-mM salt solution. As an input for v , the speed of sound in the DNA polymer (as it appears in the equation for the electric field E_z), we have used a value of 1.8×10^3 m/s, as measured by Hakim *et al.*¹¹

Equations (8) and (9) contain ω -dependent imaginary terms, arising from the frictional damping at the two interfaces. If the constants Γ and γ were simply zero, the set of equations for q_i^α and \bar{s} would reduce to a simple eigenvalue problem and could be solved by direct diagonalization of the dynamical matrix. On the other hand, one notes that the ω -dependent imaginary terms appear only

in very small part of the total equation set, that is, for the q_i^α of the phosphate group atoms and the coordinate \bar{s} , as compared to the 124 size of the full problem. In fact, since the phosphorous atoms among the phosphate group are the heaviest and have the maximum partial charges on them, one can make the very reasonable approximation that the coupling of the sheath to the DNA is confined only to the phosphorous atoms. Therefore the number of equations with ω -dependent imaginary terms is reduced to only three. This problem can be solved by a self-consistent iterative procedure.

Our equations of motion can be written as

$$-\omega^2 x_i = \sum_{j=1}^N F_{ij} x_j - i\gamma_i \omega x_i. \quad (55)$$

One can write Eq. (55) in a different form:

$$-\omega^2 \left[1 - i \frac{\gamma_i}{\omega} \right] x_i = \sum_{j=1}^N F_{ij} x_j. \quad (56)$$

Now by defining $l_i = (1 - i\gamma_i/\omega)^{1/2}$ and dividing Eq. (56) by l_i one gets

$$-\omega^2 \bar{x}_i = \sum_{j=1}^N \bar{F}_{ij} \bar{x}_j, \quad (57)$$

with $\bar{x}_i = l_i x_i$ and $\bar{F}_{ij} = F_{ij}/(l_i l_j)$. Equation (57) defines a new eigenvalue problem which can be solved by direct diagonalization of \bar{F}_{ij} . Thus an iterative procedure can be followed to solve the original problem defined in Eq. (55): One first solves the original problem with all $\gamma_i = 0$ and then uses one of the ω (corresponding to a particular branch of the vibrational spectrum) in defining l_i , which can in turn be used in Eq. (57) to define \bar{F}_{ij} . Equation (57) is then solved by diagonalization of the new matrix \bar{F}_{ij} . The solution of this is used as an input to define new l_i and thus new \bar{F}_{ij} . This defines the iterative procedure which can be repeated until reasonable convergence is obtained. The procedure must be repeated for each phonon branch of interest.

A more general form of the procedure outlined above was used to calculate the low-frequency vibrational modes of the DNA-sheath system, defined by Eqs. (8) and (9). A fast convergence, in five or six iterations, was obtained for all the low-frequency modes of interest. In Fig. 2 we present the dispersion curves for the lowest six modes of the system, as wave number versus θ , where $\theta = qa$ is the base pair-to-base pair phase angle. As is expected we get the usual four acoustic modes: one compressional, one torsional at zone center $\theta = 0$, and two bending modes at $\theta = \pm\psi$, where ψ is the pitch angle of the DNA helix. The slope of the compressional acoustic mode near the zone center ($\theta \approx 0$) yields a sound-wave speed of 1.89×10^3 m/s, in excellent agreement with the experimental value used as an input in the calculations.

Besides the four acoustic modes cited above, we also get another extra acoustic mode with a large slope at the zone center. The speed of propagation of the disturbance represented by this steep mode turns out to be 36.5×10^3 m/s. Analysis of the eigenvector of this mode shows that it consists largely of a longitudinal collective motion of the charged sheath counter to the motion of the opposite-

ly charged polymer core. Near the zone center this mode frequency has a linear dependence on wave number. From the nature of the mode and its high-speed of propagation in DNA, one can interpret this mode as a one-dimensional longitudinal plasmon mode, representing the collective motion of the free charges in the DNA-sheath system. These observations verify our conjecture about the existence of an extra acoustic mode in the DNA-sheath system.

It is instructive to examine the effect of damping on the acoustic modes, particularly comparing the DNA compressional mode and the plasmon mode. Analysis of the numerical results shows that the relative width $\Delta\omega/\omega$, for the plasmon mode, at $\theta=1^\circ$, is 0.21. On the other hand the relative width of the compressional mode turns out to be 4.86; too great to define a resonance. These data indicate that, whereas the mechanical compressional mode of the DNA is highly damped, the electrical plasmon mode is well defined, in spite of the effects of frictional damping forces at the two interfaces in the system.

V. DISCUSSION AND CONCLUSIONS

Excellent agreement of our result for the speed of sound in the DNA with its experimental value is indicative of the usefulness of the procedure used in the last three sections. It is strongly suggestive that one can very safely replace the effect of nonbonded long-range interactions by means of an effective local field arising from the motions of the DNA atoms and the counterions. This effective field approximation simplifies, to a great extent, the complications arising due to summations over 15 to 20 unit cells on each side of a central base pair in the usual treatment of the long-range forces. Further, once the summations are not needed, one can easily extend this effective field procedure to more complicated broken-symmetry problems in DNA, such as a terminus or some other defect.

The older calculation of Mei *et al.*¹ successfully gave values for the measured¹¹ sound velocity in the lower microwave portion of the spectrum; the present calculation achieves this also. Both calculations also produce the same infrared and Raman spectra. This is because the higher-frequency vibrations, falling in the 400-cm^{-1} range and up, are strongly localized and essentially independent of any long-range interactions.

The only other experimental datum useful for comparing the two calculations is Lindsay's report¹² of a mode at around 12 cm^{-1} which softens at high hydration and is thereby implicated in the water-dependent *A-B* transition. This resonance is the lowest optical mode of the spectrum in the Mei work. Referring to Fig. 2, we see that the present work also shows an optical mode at around 12 cm^{-1} . The behavior of this resonance under varying hydration cannot be usefully discussed because the long-range transverse extent of the **E** and **B** fields here restricts our results to the high-hydration, low-concentration limit. However, we note in Fig. 2 that there is a lowest mode predicted at about 3 cm^{-1} ; the 12-cm^{-1} mode is of differing character (although this can-

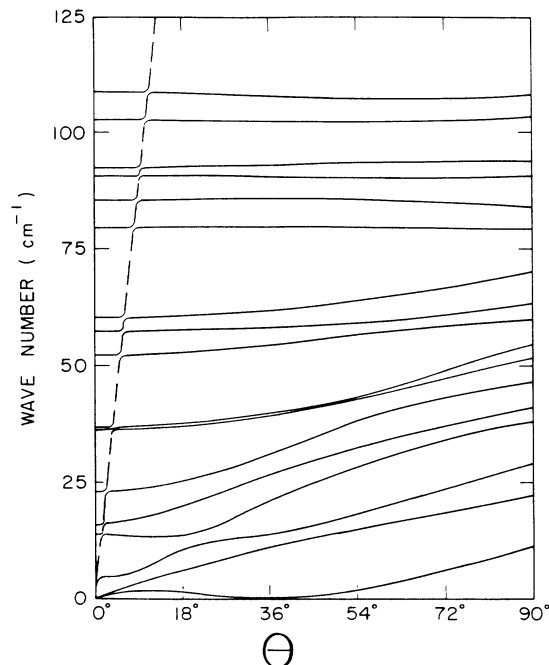


FIG. 2. Low-frequency normal mode spectrum DNA—poly(dA)-poly(dT), where *dA* refers to repeating adenine bases on one strand and *dT* the repeating thymine bases on the other strand. The lowest two phonon branches, around origin, are torsional and compressional in character. At $\theta=36^\circ$ there are two bending modes. The steepest acoustic branch, shown by a dashed line, is the DNA plasmon mode. Several low-lying optical modes are also displayed.

not be discerned just by looking at the spectrum).

Hence, the discovery of a lowest optical resonance would incontrovertably establish the current model over the older one. The frequency range $2\text{--}20\text{ cm}^{-1}$ is unfortunately an experimentally difficult one. We eagerly await news of continuing progress in this area.

A completely new feature of theory presented here is the existence of the one-dimensional plasmon mode. The appearance of this mode is strongly dependent on the assumption of a truly one-dimensional system, a DNA polymer molecule in an ocean of solvent. It is obvious that the plasmon is a property of the dissolved material. This is expected to make possible observation and identification of the DNA plasmon difficult. For small dilutions of DNA in solution, when a reasonably one-dimensional character of the dissolved molecules can be assumed, the random orientation of the molecules eliminates the possibility of an average *q* selection and makes the spectroscopic observation difficult. On the other hand, in a concentrated solution, the molecules interact and the one-dimensional nature of the dissolved material is lost. However, large electric dipole moments associated with the plasmon and its strong coupling to the electromagnetic fields are favorable aspects for a possible observation of the DNA plasmon.

In conclusion we wish to emphasize that the replacement of the long-range interactions between distant parts of the molecule by an effective local field, besides simpli-

ying the computational procedures, leads to new interesting phenomena. The effective field approach also leads to an excellent agreement with the experimentally observed sound-wave speed of the DNA. This suggests that the method can be extended to other complicated situations in the studies of the DNA. An important aspect of the theory is the form of charge distribution of the atoms, in the long-range part of the interactions within a unit cell. As mentioned earlier in the present analysis we used the absolute values of the charges; how-

ever, we are presently extending the theory to more realistic charge distributions, using algebraic values of the charges in the calculation of long-range electrostatic interactions within a unit cell or between the nearest-neighbor cells.

ACKNOWLEDGMENT

The research for this paper was performed under the office of Naval Research (ONR), Contract No. N00014-87-K-0162 funded by the SDIO.

*On leave of absence from Departamento de Física, Universidade Federal de Santa Catarina, Florianópolis, Santa Catarina, Brazil.

¹W. N. Mei, M. Kohli, E. W. Prohofsky, and L. L. Van Zandt, *Biopolymers* **20**, 833 (1981).

²B. F. Putnam, L. L. Van Zandt, E. W. Prohofsky, and W. N. Mei, *Biophys. J.* **35**, 271 (1981).

³L. L. Van Zandt and V. K. Saxena, *Phys. Rev. Lett.* **61**, 1788 (1988).

⁴B. H. Dorfman and L. L. Van Zandt, *Biopolymers* **22**, 2639 (1983).

⁵G. S. Edwards, C. C. Davis, J. D. Saffer, and M. L. Swicord, *Phys. Rev. Lett.* **53**, 1284 (1984).

⁶C. Gabriel, E. H. Grant, R. Tata, P. R. Brown, B. Gestblom,

and E. Noreland, *Nature* **328**, 145 (1987).

⁷M. E. Davis and L. L. Van Zandt, *Phys. Rev. A* **37**, 888 (1988).

⁸N. J. Tao, S. M. Lindsay, and A. Rupprecht, *Biopolymers* **26**, 171 (1987).

⁹L. L. Van Zandt, K.-C. Lu, and E. W. Prohofsky, *Biopolymers* **16**, 2481 (1977).

¹⁰W. K. Schroll, V. V. Prabhu, E. W. Prohofsky, and L. L. Van Zandt, *Biopolymers* (to be published).

¹¹M. B. Hakim, S. M. Lindsay, and J. Powell, *Biopolymers* **23**, 1185 (1984).

¹²S. M. Lindsay and J. Powell, in *Structure and Dynamics: Nucleic Acids and Proteins*, edited by E. Clementi and R. Sarma (Adenine, New York, 1983), p. 241.